J Electr Eng Technol.2017; 12(5): 1697-1708
http://doi.org/10.5370/JEET.2017.12.5.1697

ISSN(Print) 1975-0102
ISSN(Online) 2093-7423

# Identification of Inrush and Internal Fault in Indirect Symmetrical Phase Shift Transformer Using Wavelet Transform

**Shailendra Kumar Bhasker†, Manoj Tripathy* and Vishal Kumar***

**Abstract** – This paper proposes an algorithm for the differential protection of an Indirect Symmetrical Phase Shift Transformer (ISPST) by considering the different behaviors of the compensated differential current under internal fault and magnetizing inrush conditions. In this algorithm, a criterion function is defined which is based on the difference of amplitude of the wavelet transformation over a specific frequency band. The function has been used for the discrimination between three phase magnetizing inrush and internal fault condition and requires less than a quarter cycle after disturbance. This method is independent of any coefficient or threshold values of wavelet transformation. The merit of this algorithm is demonstrated by the simulation of different faults in series and excitation unit and magnetizing inrush with varying switching conditions on ISPST using PSCAD/EMTDC. Due to unavailability of in-field large interconnected transformers for such a large number of destructive tests, the results are further verified by Real Time Digital Simulator (RSCAD/RTDS). The proposed algorithm has been compared with the conventional harmonic restraint based method that justifies the application of wavelet transform for differential protection of ISPST. The proposed algorithm has also been verified for different rating of ISPSTs and satisfactory results were obtained.

**Keywords**: Differential protection, Internal fault, Magnetizing inrush current, Phase shift transformer, Wavelet transformation

## 1. Introduction

Phase Shift Transformer (PST) is an important electrical component used for the power flow control through specific line in a complex power transmission network. The basic function of the PST is to change the effective phase displacement between input and output voltage of a transmission line. Power flow control using PST is given by (1). There are different types of PST according to their construction as discussed in [1]. Indirect Symmetrical PST (ISPST) is widely used because of its simple construction as shown in Fig. 1. It helps in the utilization of power transmission lines which improve the system operating performance and efficiency.

$$p = \frac{|V_S||V_L|}{X_T}\sin(\delta \pm \Delta\theta) \quad (1)$$

where, $V_S$ and $V_L$ are source and load side voltage, δ is phase angle between $V_S$ and $V_L$, $\Delta\theta$ is change in phase angle due to ISPST.

Considering the importance and cost of an ISPST, it requires fast and reliable protection. However, there are many protection schemes such as differential protection, overload protection, over excitation protection, through current backup protection etc. [2], but differential protection is the main protection scheme which is applied for internal faults in an ISPST. In differential protection, an ISPST is protected for both the series and excitation unit [3-5]. This needs 18 CTs, 9 for each protection, which makes the protection quite costly. Furthermore, differential relay is prone to mal-operate in presence of inrush currents of an ISPST [2]. The major drawback of differential protection is the false tripping caused by these magnetizing inrush current [6]. The magnetizing inrush current generates large amount of second harmonic component in comparison to an internal fault current, which is also utilized in second harmonics restrained principle for differential protection

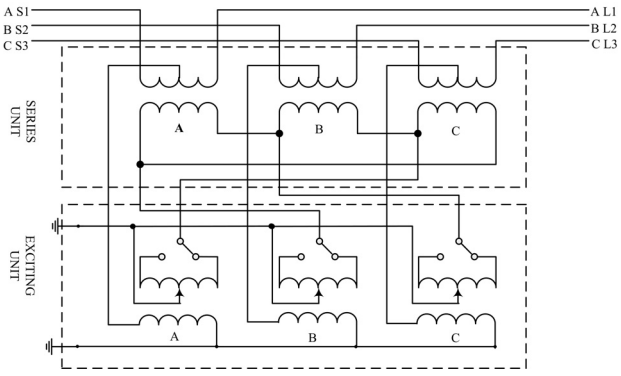


**Fig. 1.** Circuit of indirect symmetrical phase shift transformer [4]

† Corresponding Author: Dept. of Electrical Engineering, Indian Institute of Technology, Roorkee, India. (bhaskershailu@gmail.com)
* Dept. of Electrical Engineering, Indian Institute of Technology, Roorkee, India. ({manojfee, vksaxfee}@iitr.ac.in)
Received: June 7, 2016; Accepted: April 20, 2017

[3, 6-8]. However in case of extra high voltage (EHV) transmission lines and the use of high-quality, low-loss core materials in modern transformer affected the second harmonic restraint scheme [9-11]. Similar to power transformer protection, ISPST's differential protection also bring several challenges such as non-standard phase shift between two ends, turn to turn fault, saturation of the winding exposed to high voltages etc. [12-14]. Protection of PST is discussed in [15, 16], which are based on normal operating voltage-current relationship and tracking of the tap-changer position. However, the disadvantage of this technique is that it requires potential transformer and tracking device in conjunction with current transformer (CT). A lot of research has been reported for the discrimination between internal fault current and inrush current in power transformers. Several methods have been proposed to detect internal faults of the power transformer. In some methods, differential current and differential current harmonics are used as inputs to a trained neural network [17, 18]. Signal processing is also used to extract the features for the training of neural network [19]. The problem associated with these methods is the need of a large number of training patterns produced by simulations of various cases. S-transformation technique has been discussed to extract the patterns of transient signals during internal fault and inrush condition [20]. In this technique, discrimination needs one cycle samples and total operating time is 30ms approximately from the inception time of disturbance. Wavelet packet transformation (WPT) has also been discussed for certain feature extraction of the differential current [21]. However WPT based technique has not been considered for on-load inrush condition. Wavelet Transform (WT) has also been used for differential protection of power transformer [22, 23].

This paper proposes an algorithm based on WT for the discrimination between internal fault and inrush condition in different mode of operation of an ISPST. The algorithm is based on the difference of amplitudes of wavelet coefficients of compensated differential current over a specific frequency band. The internal fault and inrush condition can be discriminated accurately in less than a quarter cycle after the disturbance. ISPST's source- and load-side current data have been generated from PSCAD/ EMTDC and RSCAD/RTDS software and the saved data is used for wavelet analysis using MATLAB platform. The proposed algorithm has been compared with the conventional harmonic restraint based method to justify the application of WT. Proposed method eliminates the need of separate protection of primary and secondary winding.

## 2. Wavelet Transform

WT is a useful computational tool for a variety of transient signals [24, 25]. It allows time localization of different frequency components of a given signal, with a variable time-width windowing function. WT can separate transient components in the upper frequency isolated in a shorter part of the power frequency cycle. WT has the ability to focus on short time intervals for high frequency components and long intervals for low frequency components which increases the analysis of signals with localized impulses and oscillations. Because of this reason, wavelet decomposition is ideal for analyzing the transient signals and getting much better current characterization and is useful for reliable discrimination of internal fault current from magnetizing inrush current [26]. WT also helps to de-noise the signals at different level of wavelet decomposition. For wavelet transformation of the signal $X(t)$, the wavelet function $\psi(t)$ and scaling function $\phi(t)$ must be defined. The $\psi(t)$ serving as a high pass filter can generate the detailed version of the distorted signal, and $\phi(t)$ can generate the approximated version of the distorted signal. In general, the discrete $\psi(t)$ and $\phi(t)$ can be defined as follows [27]:

$$\psi_{j,n}(t) = 2^{j/2}\sum_{n} d_{j,n}\psi(2^{j}t-n) \tag{2}$$

$$\phi_{j,n}(t) = 2^{j/2}\sum_{n} c_{j,n}\phi(2^{j}t-n) \tag{3}$$

where, $n$ is decomposition level, $d_j$ is the wavelet coefficient and $c_j$ is the scaling coefficient at scale $j$.

Consider the original signal $X_j(t) = (x_0, x_1, ....., x_{N-1})$ at scale $j$ sampled at constant time interval, the sampling number is $N=2^J$, where J is an integer value. Its DWT is presented as follows [27]:

$$DWT(X_j(t)) = \sum_{k} X_j(t)\ \phi_{j,k}(t)dt\,, \tag{4}$$

$$= 2^{\frac{(j+1)}{2}}\left(\sum_{n} y_{j+1,n}\phi(2^{j+1}t-n)) + \sum_{n} z_{j+1,n}\psi(2^{j+1}t-n)\right),$$

$$0 \le n \le \frac{N}{2^j}-1 \tag{5}$$

where,

$$y_{j+1,n} = \sum_{k} c_{j,k}x_{j,k+2n}, \qquad 0 \le k \le \frac{N}{2^j}-1 \tag{6}$$

$$z_{j+1,n} = \sum_{k} d_{j,k}x_{j,k+2n}, \quad 0 \le k \le \frac{N}{2^j}-1 \tag{7}$$

$$d_k = (-1)^k c_{2p-1-k}, \quad p = \frac{N}{2^j} \tag{8}$$

where, $j$ is translation coefficient, $y_{j+1,n}$ is approximation version at scale $j$+1 and $z_{j+1,n}$ is detailed version at scale $j$+1.

In this paper the sampling frequency is taken to be 10 kHz and Daubechies function is selected as a mother wavelet function. Daubechies function is a better frequency extractor than Haar. This is due to its low pass and high pass

**Table 1.** Wavelet function coefficients at different frequency levels

| Frequency component (Hz) | Wavelet component |
|---|---|
| 2500-5000 | D1 |
| 1250-2500 | D2 |
| 625-1250 | D3 |
| 312.5-625 | D4 |
| 156.25-312.5 | D5 |
| 78.12-156.25 | D6 |
| 39.06-78.125 | D7 |
| 0-39.06 | A7 |

filter which resemble more ideal filters than those of Haar wavelet. On the other hand, because of its orthogonality, it satisfies Parsaval's theorem, not like biorthogonal wavelets, such as Coifet and Meyer wavelets [28]. Table 1 shows the band of frequencies at different wavelet function coefficient for sampling frequency of 10 kHz.

## 2. Proposed Algorithm

The proposed algorithm is based on the characteristic of the compensated differential current waveform for the identification of internal fault and magnetizing inrush condition in an ISPST. In case of magnetizing inrush condition, the slope of waveform increases very slowly at the time of switching after that start increasing. However in case of internal fault, slope of the waveform at the time of fault occurs, increases rapidly as shown in Fig. 2 [29]. These features of the fault and inrush current do not depend on the transformer parameter and connected power system. The technique has been discussed for the power transformer protection [23]. In case of phase shifting transformer, there are two modes of operation namely advance and retard phase shift. However, in both modes of operation of an ISPST, there is no change in the behavior of differential current, either in magnetizing inrush current or internal fault current. But magnitude and phase of differential current changes due to corresponding change in phase shift between two ends. If the scheme reported in [23] applied to ISPST, it would trip even in the case of through faults because of non-standard phase shift of an ISPST. So in this technique phase shift compensation has been incorporated to avoid mal-operation of relay due to through fault [13]. After phase shift compensation, threshold is decided as done in power transformer. The restraining currents are only used to prevent false tripping due to external fault, CTs ratio mismatch, CTs error and mismatch caused by tap changer position.

The proposed algorithm is based on the following principle:

- ✓ A large slope characteristic of the waveform in the time domain shows the presence of higher frequencies components.
- ✓ A low slope characteristic of the waveform in the time domain shows the presence of lower frequencies components.

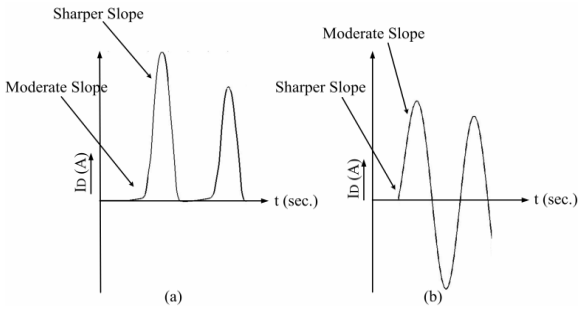


**Fig. 2.** Behavior of (a) magnetizing inrush and (b) fault

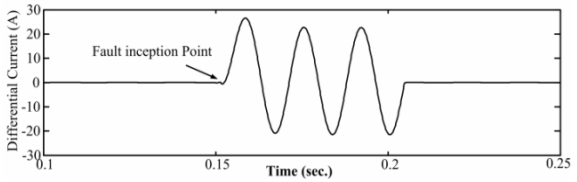


(a)

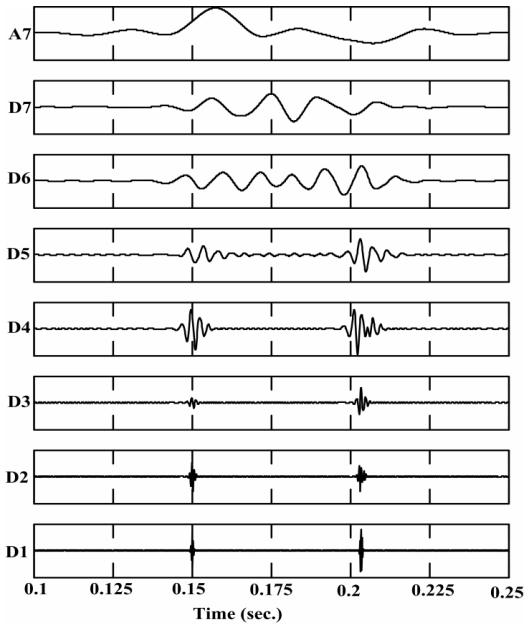


(b)

**Fig. 3.** (a) Compensated differential current due to internal A-G fault in the excitation unit primary winding at t=0.15sec. (b) Frequency levels of compensated differential current during internal fault

The effect of these frequency components can be analyzed using convolution filters. These multiband convolutions can be implemented using WT. The differentiation can be made between inrush and internal fault conditions on the basis of their WT. It is observed that in case of internal fault, the amplitude of frequencies falling in range of (D1-D4) wavelet component has decreasing tendency during

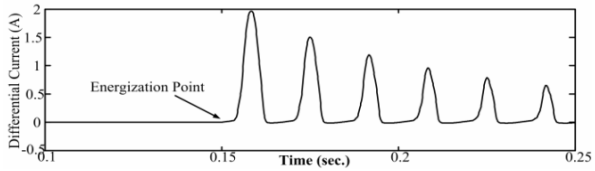


(a)

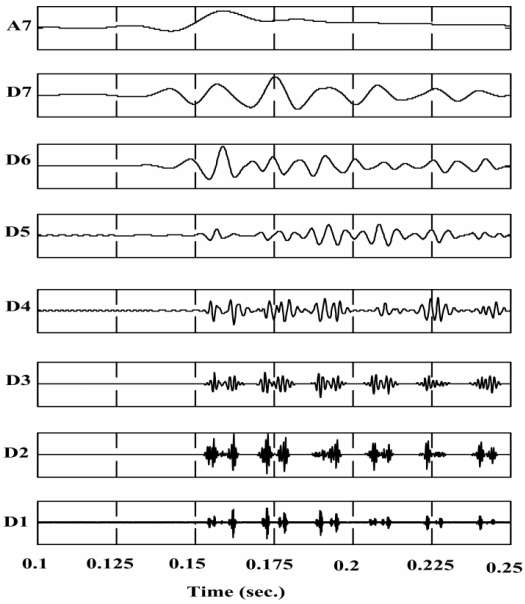


(b)

**Fig. 4.** (a) Compensated differential current due to magnetizing inrush current at t = 0.15 sec; (b) Frequency levels of compensated differential current during magnetizing inrush

the initial instants of fault. However in case of magnetizing inrush, the amplitude of frequencies has an increasing tendency during the initial instants of magnetization. Fig. 3(a) shows the compensated differential current in case of phase A to ground fault in excitation unit primary winding occurring at t=0.15sec. and tendency is shown (D1-D4) in Fig. 3(b). Similarly for the magnetizing inrush current at switching time t=0.15sec. shown in Fig. 4(a) and tendency is shown (D1-D4) in Fig. 4(b).

The above mentioned features diminish with the decrease in frequency level. WT coefficient D4 gives distinct response with high magnitude as compare to D1-D3. In order to develop a criterion function for discriminating the inrush current from internal fault current, the amplitude of the first two peaks (termed as X and Y) of the compensated differential current in D4, following the disturbance, are considered. When WT is determined for the samples available in the window length, the window updates its samples after every sampling time period. After getting the WT of data available in window, |D4| coefficient of WT will processed to measure the first two peaks (X and Y). If an element of |D4| data is larger than both of its neighbors or equals, the element is a first peak (X). Similar process

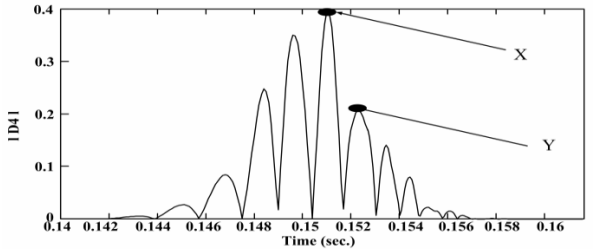


(a)

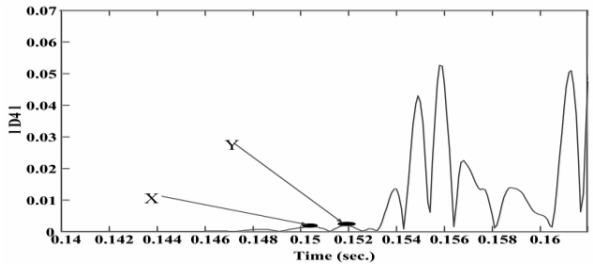


(b)

**Fig. 5.** Absolute value of D4 for (a) internal fault; (b) magnetizing inrush

is used to find second peak (Y). The magnitude of compensated differential current in its WT coefficient |D4| and points X and Y are shown in Fig. 5(a) and (b) for internal fault and magnetizing inrush respectively. It can be observed that, in the case of inrush current X<Y i.e. X–Y is negative (–ve), where as in the case of internal fault X>Y i.e. X–Y is positive (+ve). The internal fault is studied for every phase and depending on the sign of X–Y (+ve or –ve), the trip command is issued. The sign of X–Y (+ve or –ve) discriminates the inrush current from internal fault with in a quarter cycle. Therefore proposed algorithm does not require any threshold value of WT for the discrimination between internal fault and inrush condition. The classification is solely based on the sign of value of (X-Y). The proposed algorithm is more suitable when applied to different ratings of ISPST since it is independent of any threshold.

A flow chart for the proposed algorithm is shown in Fig. 6 and describe that after measuring the current from source- and load-side CTs of ISPST, the block-(B) performs the phase compensation for the compensation of non-standard phase shift. In block-(C) anti-aliasing filter is used to restrict the bandwidth of a signal to approximately or completely satisfy the sampling theorem and then sampling have been done at 10 kHz sampling frequency. Block-(D) calculates the compensated differential current and restraining current of each phase from the CTs. In block-(E), the restraining currents are used prevent the mal-operation during external fault, CT miss-match, CT ratio error and CT saturation during external fault. Hence, the pickup value is decided with the consideration of these factors. If the magnitude of the compensated differential current is greater than pickup value, then either there is an

inrush current and/or internal fault current. If the output is 'No' then calculate three phase differential current again. In block-(F), wavelet transformation of the differential current starts using sliding window. Sliding window has pre-fault and post fault data to get better resolution of post-fault data during wavelet transform. After wavelet transform, |D4| frequency coefficient of wavelet transform is considered for the comparison of its consecutive peaks. The value of X and Y of |D4| is measured for each phase in block-(G). At the end of the algorithm decision making block-(H) discriminates internal fault condition from inrush condition where 'a', 'b', and 'c' stands for phase a, phase b, and phase c respectively. If the block-(H) gives output as 'No', then again calculate three phase differential current, if output is 'Yes', a trip signal will be issued to the circuit breaker.

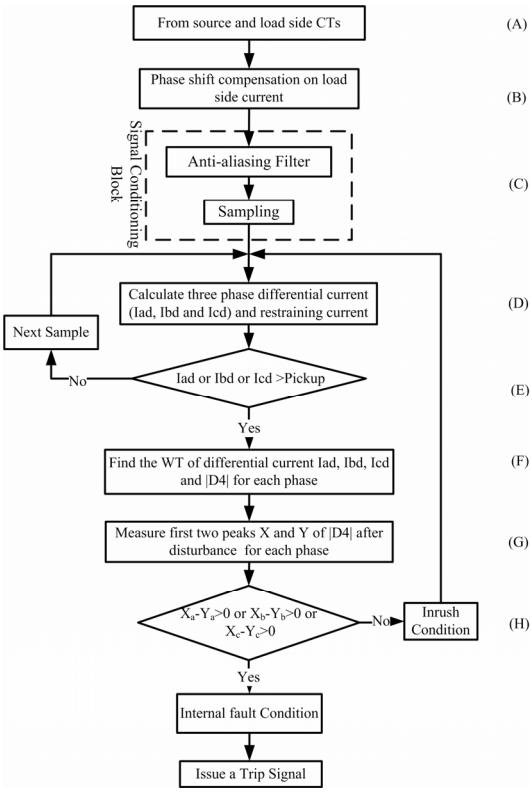


**Fig. 6.** Flowchart of the proposed algorithm

## 4. Simulation and Results

The proposed approach has been evaluated for various operating conditions of an ISPST. ISPST model is simulated in PSCAD/EMTDC whose connection is discussed in [30]. Compensated differential currents are obtained for each phase with star connected CTs on both sides of the ISPST using PSCAD/EMTDC. The line diagram is shown in Fig. 7. Two different rating ISPSTs have been used for the illustration of the proposed algorithm.

**A. System 1**: 300MVA, 138kV/138kV, 1255A/1255A, 60 Hz ISPST with maximum phase shift of ±30° and

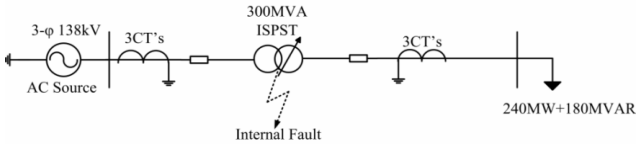


**Fig. 7.** Line diagram of simulated model

**Table 2.** Values of X and Y ($\times 10^{-3}$) for each phase compensated differential current for magnetizing inrush current

| % Residual flux | Switching angle (θ) | Phase | Retard Phase Shift | | | | | | Advanced Phase Shift | | | | | |
|---|---|---|---|---|---|---|---|---|---|---|---|---|---|---|
| | | | On Load | | | No Load | | | On Load | | | No Load | | |
| | | | X | Y | X-Y | X | Y | X-Y | X | Y | X-Y | X | Y | X-Y |
| 0% | 0° | a | 10.38 | 35.52 | –ve | 1.455 | 1.924 | –ve | 56.44 | 84.6 | –ve | 23.73 | 35.23 | –ve |
| | | b | 36.72 | 41.11 | –ve | 9.654 | 21.47 | –ve | 14.55 | 15.41 | –ve | 5.392 | 7.831 | –ve |
| | | c | 8.686 | 10.85 | –ve | 4.316 | 5.883 | –ve | 18.93 | 25.62 | –ve | 4.995 | 9.857 | –ve |
| | 60° | a | 21.45 | 21.62 | –ve | 6.149 | 20.11 | –ve | 7.042 | 9.948 | –ve | 5.957 | 16.32 | –ve |
| | | b | 3.83 | 51.39 | –ve | 1.807 | 2.389 | –ve | 4.824 | 5.932 | –ve | 1.494 | 4.261 | –ve |
| | | c | 6.312 | 10.29 | –ve | 0.940 | 2.88 | –ve | 9.641 | 25.05 | –ve | 5.792 | 12.73 | –ve |
| | 90° | a | 35.52 | 51.87 | –ve | 6.39 | 24.13 | –ve | 2.691 | 3.243 | –ve | 1.145 | 7.580 | –ve |
| | | b | 23.15 | 37.46 | –ve | 3.807 | 5.601 | –ve | 6.794 | 17.59 | –ve | 2.81 | 14.20 | –ve |
| | | c | 8.686 | 10.85 | –ve | 2.308 | 13.63 | –ve | 32.91 | 37.95 | –ve | 11.31 | 39.74 | –ve |
| 50% | 0° | a | 22.29 | 24.96 | –ve | 17.34 | 53.49 | –ve | 3.11 | 8.675 | –ve | 22.11 | 33.26 | –ve |
| | | b | 4.731 | 4.925 | –ve | 7.165 | 11.41 | –ve | 10.16 | 11.90 | –ve | 0.994 | 9.321 | –ve |
| | | c | 8.301 | 23.71 | –ve | 12.12 | 12.92 | –ve | 38.6 | 60.88 | –ve | 10.06 | 10.81 | –ve |
| | 60° | a | 8.70 | 9.898 | –ve | 21.49 | 25.11 | –ve | 62.94 | 85.39 | –ve | 45.79 | 53.08 | –ve |
| | | b | 4.295 | 7.180 | –ve | 2.785 | 15.63 | –ve | 26.32 | 31.25 | –ve | 1.108 | 1.351 | –ve |
| | | c | 5.495 | 6.949 | –ve | 13.37 | 23.21 | –ve | 11.79 | 19.51 | –ve | 6.412 | 8.516 | –ve |
| 80% | 0° | a | 48.57 | 49.76 | –ve | 11.57 | 45.78 | –ve | 28.31 | 33.22 | –ve | 27.26 | 46.07 | –ve |
| | | b | 1.74 | 12.31 | –ve | 13.8 | 24.86 | –ve | 10.07 | 24.48 | –ve | 8.052 | 23.19 | –ve |
| | | c | 49.19 | 53.47 | –ve | 30.17 | 34.4 | –ve | 46.73 | 48.06 | –ve | 12.26 | 14.67 | –ve |
| | 60° | a | 68.96 | 93.70 | –ve | 14.80 | 24.0 | –ve | 4.389 | 34.09 | –ve | 41.86 | 46.71 | –ve |
| | | b | 5.899 | 19.24 | –ve | 3.95 | 7.50 | –ve | 40.25 | 58.61 | –ve | 10.59 | 24.14 | –ve |
| | | c | 28.47 | 43.95 | –ve | 2.39 | 10.40 | –ve | 5.293 | 8.354 | –ve | 0.699 | 2.309 | –ve |
| | 90° | a | 27.04 | 40.97 | –ve | 35.06 | 47.65 | –ve | 52.06 | 76.63 | –ve | 49.25 | 68.70 | –ve |
| | | b | 9.963 | 14.56 | –ve | 22.97 | 64.47 | –ve | 26.91 | 30.54 | –ve | 10.94 | 17.83 | –ve |
| | | c | 1.556 | 2.09 | –ve | 18.51 | 24.82 | –ve | 21.8 | 21.89 | –ve | 15.61 | 22.00 | –ve |

**Table 3.** Values of X and Y ($\times 10^{-2}$) for each phase compensated differential current for different internal fault cases in excitation unit

| Fault Inception Angle | Type of Fault | Phase | Excitation unit fault | | | | | | | | | | | |
|---|---|---|---|---|---|---|---|---|---|---|---|---|---|---|
| | | | Retard phase shift | | | | | | Advance phase shift | | | | | |
| | | | On-Load | | | No-Load | | | On-Load | | | No-Load | | |
| | | | X | Y | X-Y | X | Y | X-Y | X | Y | X-Y | X | Y | X-Y |
| 0° | A-G | a | 39.62 | 20.77 | +ve | 39.82 | 20.35 | +ve | 25.28 | 14.26 | +ve | 21.79 | 12.22 | +ve |
| | | b | 6.804 | 3.406 | +ve | 7.055 | 3.59 | +ve | 1.632 | 1.514 | +ve | 2.730 | 1.529 | +ve |
| | | c | 4.928 | 2.464 | +ve | 5.184 | 2.638 | +ve | 2.291 | 2.188 | +ve | 3.734 | 2.098 | +ve |
| | A-B | a | 38.35 | 27.85 | +ve | 25.61 | 24.76 | +ve | 17.58 | 15.08 | +ve | 53.23 | 24.68 | +ve |
| | | b | 79.52 | 39.86 | +ve | 26.46 | 14.38 | +ve | 129.7 | 67.73 | +ve | 71.41 | 26.58 | +ve |
| | | c | 8.623 | 5.502 | +ve | 7.342 | 3.231 | +ve | 12.79 | 6.147 | +ve | 18.15 | 8.943 | +ve |
| | A-B-G | a | 244.9 | 68.61 | +ve | 39.21 | 32.83 | +ve | 120.1 | 71.54 | +ve | 21.36 | 17.30 | +ve |
| | | b | 37.07 | 16.84 | +ve | 84.12 | 41.68 | +ve | 46.74 | 35.25 | +ve | 119.8 | 63.80 | +ve |
| | | c | 28.91 | 5.491 | +ve | 9.586 | 6.367 | +ve | 42.88 | 10.00 | +ve | 15.40 | 7.793 | +ve |
| | A-B-C | a | 19.95 | 12.80 | +ve | 32.14 | 16.48 | +ve | 15.47 | 13.18 | +ve | 19.75 | 15.09 | +ve |
| | | b | 80.77 | 39.52 | +ve | 83.93 | 39.14 | +ve | 109.9 | 63.03 | +ve | 99.99 | 58.15 | +ve |
| | | c | 128.0 | 60.47 | +ve | 120.5 | 54.96 | +ve | 99.48 | 48.71 | +ve | 93.86 | 46.18 | +ve |
| 60° | A-G | a | 144.0 | 67.22 | +ve | 60.16 | 37.02 | +ve | 144.0 | 67.16 | +ve | 76.92 | 49.36 | +ve |
| | | b | 13.78 | 10.57 | +ve | 10.76 | 6.541 | +ve | 13.78 | 10.57 | +ve | 10.09 | 6.410 | +ve |
| | | c | 19.36 | 14.45 | +ve | 12.35 | 7.853 | +ve | 19.36 | 14.14 | +ve | 13.79 | 8.189 | +ve |
| | A-B | a | 99.06 | 61.62 | +ve | 115.4 | 66.05 | +ve | 41.53 | 27.91 | +ve | 48.45 | 31.76 | +ve |
| | | b | 82.59 | 52.70 | +ve | 103.6 | 101.4 | +ve | 56.86 | 39.12 | +ve | 65.87 | 42.08 | +ve |
| | | c | 14.75 | 8.940 | +ve | 29.31 | 14.47 | +ve | 26.78 | 18.81 | +ve | 17.51 | 11.46 | +ve |
| | A-B-G | a | 95.54 | 55.46 | +ve | 111.9 | 60.91 | +ve | 126.2 | 63.12 | +ve | 114.0 | 77.34 | +ve |
| | | b | 149.4 | 86.63 | +ve | 132.8 | 102.4 | +ve | 43.48 | 32.25 | +ve | 95.14 | 50.65 | +ve |
| | | c | 25.60 | 15.4 | +ve | 30.11 | 14.21 | +ve | 18.60 | 11.00 | +ve | 30.91 | 17.49 | +ve |
| | A-B-C | a | 99.93 | 60.58 | +ve | 116.4 | 112.3 | +ve | 62.78 | 48.32 | +ve | 112.5 | 76.59 | +ve |
| | | b | 87.40 | 52.06 | +ve | 103.8 | 58.05 | +ve | 47.14 | 35.47 | +ve | 103.1 | 54.72 | +ve |
| | | c | 39.35 | 17.54 | +ve | 36.36 | 15.95 | +ve | 13.15 | 11.36 | +ve | 37.14 | 20.30 | +ve |
| 90° | A-G | a | 120.3 | 53.40 | +ve | 124.4 | 52.21 | +ve | 151.1 | 52.90 | +ve | 118.6 | 48.64 | +ve |
| | | b | 20.58 | 9.516 | +ve | 22.02 | 9.149 | +ve | 14.77 | 6.609 | +ve | 15.27 | 6.330 | +ve |
| | | c | 14.86 | 6.988 | +ve | 16.07 | 6.78 | +ve | 20.31 | 9.005 | +ve | 20.95 | 8.709 | +ve |
| | A-B-G | a | 172.9 | 73.89 | +ve | 180.7 | 83.57 | +ve | 111.2 | 50.74 | +ve | 116.8 | 49.26 | +ve |
| | | b | 51.96 | 26.59 | +ve | 55.88 | 22.05 | +ve | 19.69 | 14.15 | +ve | 23.08 | 11.69 | +ve |
| | | c | 23.19 | 9.537 | +ve | 23.92 | 10.53 | +ve | 22.08 | 9.180 | +ve | 21.79 | 8.803 | +ve |
| | A-B-C-G | a | 164.2 | 67.68 | +ve | 170.0 | 75.62 | +ve | 110.1 | 49.32 | +ve | 156.5 | 48.24 | +ve |
| | | b | 54.20 | 25.33 | +ve | 59.53 | 25.14 | +ve | 46.42 | 18.91 | +ve | 51.05 | 19.02 | +ve |
| | | c | 52.46 | 34.40 | +ve | 51.25 | 27.28 | +ve | 70.81 | 31.95 | +ve | 73.47 | 42.94 | +ve |

maximum loading of 240MW and 180 MVAR is taken for the application of the proposed algorithm. Relevant CTs with turn ratio 2000A/1A are connected in star on both the sides. Compensated differential current is sampled at frequency of 10 kHz.

Different cases of magnetizing inrush current with different switching angle have been studied. The residual core flux of transformer in case of no-load and on-load condition has also taken in to consideration. Similarly, different types of internal fault currents have been studied with different fault inception angles for both the retard and the advance phase shift at no-load and on-load conditions. All the cases were evaluated by the proposed algorithm as mentioned in the flow chart in Fig. 6. The results for different conditions of magnetizing inrush current have been summarized in Table 2 with their notations of (X–Y). Table 3, 4 and 5 summarize different internal fault condition in excitation unit, series unit secondary and series unit primary respectively. The case of simultaneous internal fault and inrush condition is also discussed in Table 6.

Out of these cases, some of the cases are discussed in this paper. Fig. 8 (a), (b) and (c) show the compensated differential current and its WT coefficient |D4| for A-G fault in excitation unit primary winding, A-B-G fault in series unit secondary winding and A-B-C fault in series unit secondary winding respectively at time t=0.15 sec. From Fig. 8, it is clear that the value of (X-Y) is +ve for all the three internal faults condition and hence are classified as internal fault suggested by proposed algorithm. Time axis of the WT coefficient |D4| reveals that time taken for the decision is less than a quarter cycle after disturbance occurs. There are some other possible fault conditions, which are not shown in this paper such as B-G, B-C, B-C-G etc. have symmetry with other fault condition such as A-G, A-B, A-B-G respectively shown in paper.

***Case I)*** *Effect of high impedance fault*

The technique has been extensively tested for different fault resistance (10Ω, 50Ω, 100Ω, 300Ω, 600Ω). As shown in Fig. 9, the technique discriminates, A-G fault in primary winding of excitation unit through a fault resistance of 600Ω, correctly. Fig. 9 shows the compensated differential current of phase 'a' and WT coefficient |D4|. In this case

**Table 4.** Values of X and Y ($\times 10^{-2}$) for each phase compensated differential current for different internal fault cases in series unit secondary

| Fault inception angle | Type of fault | Phase | Series unit secondary fault | | | | | | | | | | | |
|---|---|---|---|---|---|---|---|---|---|---|---|---|---|---|
| | | | Retard phase shift | | | | | | Advance phase shift | | | | | |
| | | | On-Load | | | No-Load | | | On-Load | | | No-Load | | |
| | | | X | Y | X-Y | X | Y | X-Y | X | Y | X-Y | X | Y | X-Y |
| 0° | A-G | a | 3.480 | 1.646 | +ve | 3.248 | 1.521 | +ve | 1.183 | 0.518 | +ve | 2.147 | 1.017 | +ve |
| | | b | 4.291 | 1.970 | +ve | 4.778 | 2.224 | +ve | 0.246 | 0.139 | +ve | 0.122 | .0621 | +ve |
| | | c | 15.95 | 7.420 | +ve | 15.61 | 7.360 | +ve | 12.38 | 5.870 | +ve | 13.97 | 6.621 | +ve |
| | A-B | a | 7.146 | 3.407 | +ve | 8.503 | 4.08 | +ve | 3.127 | 1.545 | +ve | 2.57 | 1.21 | +ve |
| | | b | 12.47 | 6.09 | +ve | 13.39 | 6.50 | +ve | 16.0 | 7.54 | +ve | 17.07 | 8.009 | +ve |
| | | c | 5.33 | 2.262 | +ve | 5.008 | 2.44 | +ve | 12.74 | 5.928 | +ve | 14.64 | 6.88 | +ve |
| | A-B-G | a | 9.349 | 4.376 | +ve | 10.30 | 4.88 | +ve | 3.442 | 1.691 | +ve | 3.003 | 1.419 | +ve |
| | | b | 8.826 | 4.360 | +ve | 10.45 | 5.116 | +ve | 15.0 | 7.08 | +ve | 15.88 | 7.486 | +ve |
| | | c | 10.98 | 5.164 | +ve | 10.37 | 4.852 | +ve | 13.97 | 6.516 | +ve | 16.16 | 7.584 | +ve |
| | A-B-C | a | 4.168 | 2.362 | +ve | 1.568 | 1.456 | +ve | 0.99 | 0.738 | +ve | 1.784 | 1.53 | +ve |
| | | b | 14.04 | 6.654 | +ve | 15.46 | 7.343 | +ve | 14.75 | 6.984 | +ve | 15.63 | 7.429 | +ve |
| | | c | 18.24 | 8.607 | +ve | 17.07 | 8.058 | +ve | 14.68 | 6.959 | +ve | 17.3 | 8.166 | +ve |
| 60° | A-G | a | 0.917 | 0.655 | +ve | 0.669 | 0.514 | +ve | 0.279 | 0.174 | +ve | 0.427 | 0.385 | +ve |
| | | b | 1.516 | 0.995 | +ve | 1.021 | 0.776 | +ve | 0.084 | 0.047 | +ve | 0.034 | 0.027 | +ve |
| | | c | 4.48 | 3.249 | +ve | 3.347 | 2.46 | +ve | 2.747 | 1.687 | +ve | 2.729 | 2.493 | +ve |
| | A-B | a | 9.004 | 4.936 | +ve | 7.261 | 4.730 | +ve | 0.844 | 0.55 | +ve | 1.028 | 0.679 | +ve |
| | | b | 12.21 | 7.84 | +ve | 11.66 | 7.584 | +ve | 5.692 | 3.922 | +ve | 6.794 | 4.592 | +ve |
| | | c | 4.227 | 2.955 | +ve | 4.358 | 2.832 | +ve | 5.09 | 3.34 | +ve | 5.77 | 3.88 | +ve |
| | A-B-G | a | 7.304 | 4.531 | +ve | 6.455 | 4.281 | +ve | 0.44 | 0.279 | +ve | 0.14 | 0.120 | +ve |
| | | b | 13.4 | 8.57 | +ve | 13.07 | 8.354 | +ve | 9.059 | 6.041 | +ve | 10.28 | 6.80 | +ve |
| | | c | 2.54 | 1.957 | +ve | 2.005 | 1.514 | +ve | 1.43 | 1.37 | +ve | 1.887 | 1.731 | +ve |
| | A-B-C | a | 1.65 | 0.978 | +ve | 1.374 | 1.062 | +ve | 0.738 | 0.48 | +ve | 1.419 | 1.088 | +ve |
| | | b | 3.944 | 1.283 | +ve | 4.32 | 1.33 | +ve | 4.12 | 1.223 | +ve | 4.201 | 1.272 | +ve |
| | | c | 5.289 | 1.911 | +ve | 5.001 | 1.854 | +ve | 4.364 | 1.55 | +ve | 5.043 | 1.854 | +ve |
| 90° | A-G | a | 0.454 | 0.386 | +ve | 1.937 | 0.871 | +ve | 1.423 | 1.092 | +ve | 1.937 | 0.871 | +ve |
| | | b | 0.467 | 0.308 | +ve | 0.104 | 0.049 | +ve | 0.226 | 0.208 | +ve | 0.104 | 0.049 | +ve |
| | | c | 1.659 | 1.254 | +ve | 12.56 | 5.662 | +ve | 12.09 | 5.318 | +ve | 12.56 | 5.662 | +ve |
| | A-B-G | a | 5.937 | 2.401 | +ve | 2.083 | 0.975 | +ve | 2.387 | 1.050 | +ve | 2.083 | 0.975 | +ve |
| | | b | 17.65 | 7.315 | +ve | 7.995 | 3.505 | +ve | 6.287 | 2.786 | +ve | 7.995 | 3.505 | +ve |
| | | c | 1.857 | 1.116 | +ve | 6.715 | 3.522 | +ve | 6.725 | 3.353 | +ve | 6.715 | 3.522 | +ve |
| | A-B-C-G | a | 21.63 | 9.185 | +ve | 19.04 | 8.025 | +ve | 21.25 | 8.847 | +ve | 19.04 | 8.025 | +ve |
| | | b | 11.40 | 4.998 | +ve | 7.292 | 2.860 | +ve | 9.261 | 3.993 | +ve | 7.292 | 2.860 | +ve |
| | | c | 10.66 | 5.646 | +ve | 11.98 | 5.324 | +ve | 12.37 | 5.780 | +ve | 11.98 | 5.324 | +ve |

**Table 5.** Values of X and Y ($\times 10^{-2}$) for each phase compensated differential current for different internal fault cases in series unit primary

| Fault inception angle | Type of fault | Phase | Series Unit Primary Fault | | | | | | | | | | | |
|---|---|---|---|---|---|---|---|---|---|---|---|---|---|---|
| | | | Retard phase shift | | | | | | Advance phase shift | | | | | |
| | | | On-Load | | | No-Load | | | On-Load | | | No-Load | | |
| | | | X | Y | X-Y | X | Y | X-Y | X | Y | X-Y | X | Y | X-Y |
| 0° | A-G | a | 55.91 | 31.19 | +ve | 53.84 | 30.17 | +ve | 97.14 | 93.12 | +ve | 93.57 | 79.36 | +ve |
| | | b | 5.440 | 3.180 | +ve | 6.63 | 3.618 | +ve | 2.460 | 1.45 | +ve | 2.40 | 1.47 | +ve |
| | | c | 5.20 | 2.90 | +ve | 4.80 | 2.70 | +ve | 1.470 | 1.174 | +ve | 1.68 | 1.478 | +ve |
| | A-B | a | 3.029 | 1.508 | +ve | 2.019 | 1.046 | +ve | 3.049 | 1.517 | +ve | 3.694 | 1.804 | +ve |
| | | b | 8.032 | 3.776 | +ve | 8.528 | 4.055 | +ve | 5.130 | 2.420 | +ve | 5.756 | 2.726 | +ve |
| | | c | 11.10 | 5.228 | +ve | 10.69 | 5.02 | +ve | 8.252 | 3.897 | +ve | 9.376 | 4.469 | +ve |
| 60° | A-G | a | 195.7 | 136.3 | +ve | 208.7 | 140.4 | +ve | 589.2 | 145.4 | +ve | 589.1 | 149.1 | +ve |
| | | b | 27.45 | 17.44 | +ve | 26.45 | 17.55 | +ve | 8.754 | 2.698 | +ve | 7.023 | 2.302 | +ve |
| | | c | 18.76 | 12.36 | +ve | 19.27 | 12.75 | +ve | 9.156 | 3.54 | +ve | 10.07 | 2.650 | +ve |
| | A-B | a | 3.630 | 2.098 | +ve | 3.433 | 2.124 | +ve | 4.466 | 2.65 | +ve | 4.589 | 2.826 | +ve |
| | | b | 4.620 | 2.910 | +ve | 3.87 | 2.532 | +ve | 2.620 | 1.610 | +ve | 2.965 | 1.963 | +ve |
| | | c | 1.110 | 0.770 | +ve | 0.659 | 0.577 | +ve | 1.805 | 1.119 | +ve | 1.66 | 1.583 | +ve |
| 90° | A-G | a | 189.0 | 87.96 | +ve | 211.2 | 87.44 | +ve | 176.5 | 85.94 | +ve | 197.5 | 84.44 | +ve |
| | | b | 35.3 | 14.74 | +ve | 37.28 | 15.44 | +ve | 25.08 | 10.34 | +ve | 25.75 | 10.72 | +ve |
| | | c | 25.66 | 10.82 | +ve | 27.20 | 11.27 | +ve | 34.48 | 14.18 | +ve | 35.31 | 14.70 | +ve |
| | A-B-G | a | 286.2 | 214.3 | +ve | 325.6 | 231.9 | +ve | 408.7 | 278.2 | +ve | 453.2 | 298.9 | +ve |
| | | b | 338.1 | 235.9 | +ve | 372.8 | 252.9 | +ve | 349.9 | 232.2 | +ve | 397.7 | 253.1 | +ve |
| | | c | 48.39 | 31.30 | +ve | 47.42 | 32.56 | +ve | 58.18 | 35.53 | +ve | 57.66 | 37.19 | +ve |

$X=0.49\times10^{-2}$ ($t_X=0.1502$sec.) and $Y=0.291\times10^{-2}$ ($t_Y=0.1511$sec.), i.e. X–Y=+ve. Time taken for decision is $t_d=t_Y-t_X$ (0.0009sec.). This time is less than a quarter cycle after disturbance (at t=0.15sec) so the relay will take decision before a quarter cycle after the disturbance occur.

**B. System 2:** 1400MVA, 400kV/400kV, 2020A/2020A,

60 Hz ISPST with a maximum phase shift of ±25° and maximum loading of 1120MW and 840 MVAR. Relevant CTs of turn ratio 3000A/1A are connected in star on both the sides. The compensated differential current is sampled at frequency of 10 kHz. The collected differential current data are applied to the proposed algorithm. The following cases are discussed:

***Case 1**: Turn to turn fault current*

Fig. 10(a) shows the differential current of phase 'a' and its frequency component |D4| for turn to turn (2% from neutral point) fault occurs in series unit primary winding of ISPST at on-load with retard phase shift condition. As seen from $X=1.582\times10^{-2}$ ($t_X$=0.151sec.) and $Y=0.7289\times10^{-2}$ ($t_Y$=0.152 sec.), i.e. X–Y= +ve. Time taken for the decision is $t_d=t_X-t_Y$ (0.001sec.) which is less than a quarter cycle after the disturbance.

**Table 6.** Values of X and Y($\times10^{-2}$) for each phase compensated differential current for simultaneous magnetizing inrush and internal fault

| Switching angle | Phase | Retard Phase Shift | | | Advance Phase shift | | |
|---|---|---|---|---|---|---|---|
| | | X | Y | X-Y | X | Y | X-Y |
| 0° | a | 39.70 | 20.28 | +ve | 22.62 | 12.25 | +ve |
| | b | 6.568 | 3.527 | +ve | 2.936 | 1.601 | +ve |
| | c | 5.311 | 2.957 | +ve | 4.103 | 2.053 | +ve |
| 60° | a | 59.35 | 36.75 | +ve | 76.45 | 49.17 | +ve |
| | b | 11.00 | 6.757 | +ve | 9.795 | 6.264 | +ve |
| | c | 8.292 | 5.137 | +ve | 15.21 | 10.92 | +ve |

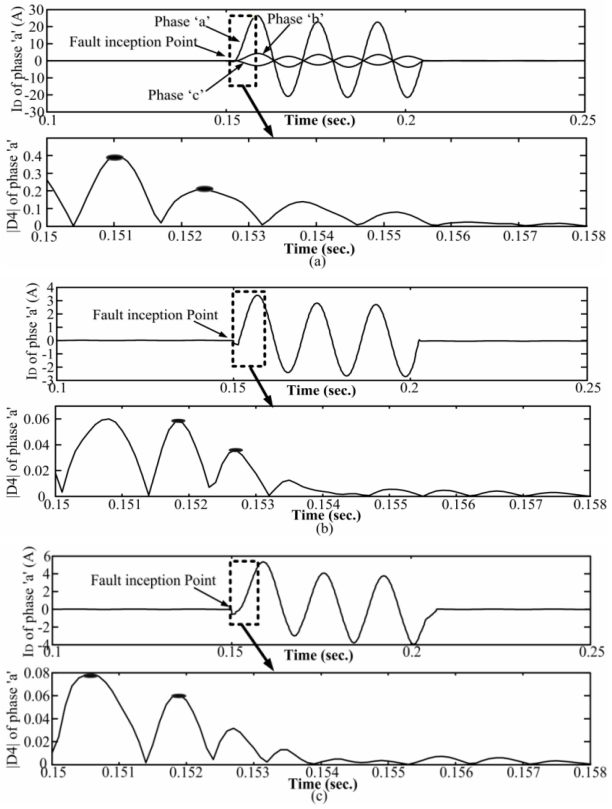


**Fig. 8.** Compensated differential fault current of phase 'a' and its WT coefficient |D4| at on-load in case of retard phase shift for (a) A-G fault in Excitation unit primary; (b) A-B-G fault in series unit secondary; (c) A-B-C fault in series unit secondary at t=0.15 sec

***Case 2**: Phase to phase fault current*

Fig. 10(b) shows the differential current of phase 'a' and its frequency component |D4| for the A-B fault in series unit primary side of ISPST at no-load with advance phase

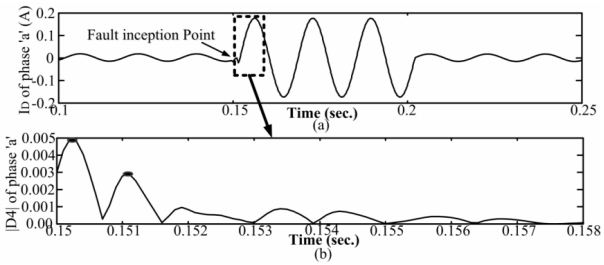


**Fig. 9.** (a) Compensated differential Fault current of phase 'a' for A-G fault in excitation unit primary winding through 600 ohm fault resistance; (b) its WT coefficient |D4| from t=.15 sec. in case of retard phase shift.

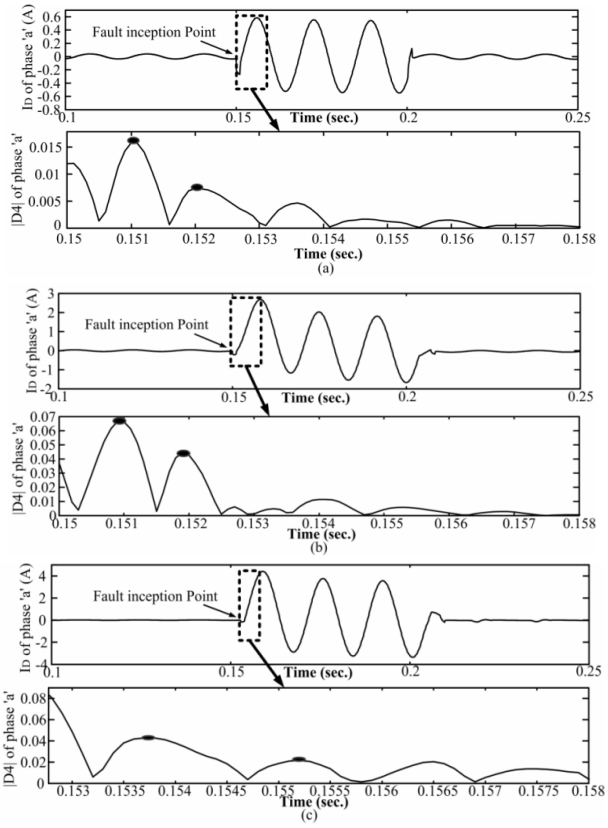


**Fig. 10.** Compensated differential current of phase 'a' and its WT coefficient |D4| at on-load for (a) turn to turn fault in series unit primary in case of retard phase shift; (b) A-B fault in series unit primary in case of advance phase shift; (c) A-B-C fault in series unit secondary in case of retard phase shift

shift condition. In this case X=$6.631\times10^{-2}$ ($t_X$=0.151sec.) and Y=$4.465\times10^{-2}$ ($t_Y$=0.0.152sec.), i.e. X–Y= +ve. Time taken for decision is $t_d = t_Y - t_X$ (0.002sec.). This time is less than a quarter cycle after disturbance so the relay will trip before quarter a cycle.

***Case 3**: Three phase fault current*

In case of three phase (A-B-C) fault in series unit secondary winding, an ISPST is on-load with retard phase shift. Fig. 10(c) shows the differential current of phase 'b' and its frequency component |D4|. In this case X= $4.262\times10^{-2}$ ($t_X$=0.1537sec.) and Y=$2.151\times10^{-2}$ ($t_Y$=0.1552 sec.), i.e. X–Y= +ve. Time taken for decision is $t_d = t_Y - t_X$ (0.0015sec.). This time is less than a quarter cycle after disturbance (t=0.1527sec.) so the relay will trip before quarter cycle.

***Case 4**: No-load magnetizing inrush current*

In case of magnetizing inrush current, no-load ISPST is switched on at t=0.15sec. In case of retard phase shift, Fig. 11 shows the differential current of phase 'a' and frequency component |D4|. In this case X=$2.06\times10^{-3}$ ($t_X$=0.1517sec.) and Y= $2.88\times10^{-2}$ ($t_Y$=0.153sec.), i.e. X–Y= –ve. Time taken for decision is $t_d = t_Y - t_X$ (0.0013sec.). This time is less than a quarter cycle after disturbance so the relay will trip before quarter a cycle.

***Case 5**: Magnetization and internal fault occurring simultaneously*

In case of simultaneous magnetizing inrush and internal fault at t=0.1527 sec. Fig. 12(a) shows differential current of phase 'a' and phase 'b' and Fig. 12(b) shows its frequency component |D4|. In this case X= $55.53\times10^{-2}$ ($t_X$=0.1537 sec.) and Y= $38.40\times10^{-2}$ ($t_Y$=0.1555 sec.), i.e. X–Y=+ve. Time taken for decision is $t_d = t_Y - t_X$ (0.0018 sec.). It is clear that the relay is operated within quarter cycle. The algorithm detects it as a fault condition for the operation of the relay.

### *C. Verification of the proposed algorithm using RSCAD/ RTDS environment*

It is not possible to perform destructive tests with in-field large interconnected ISPSTs. The proposed algorithm has been verified for system '1' using the data generated

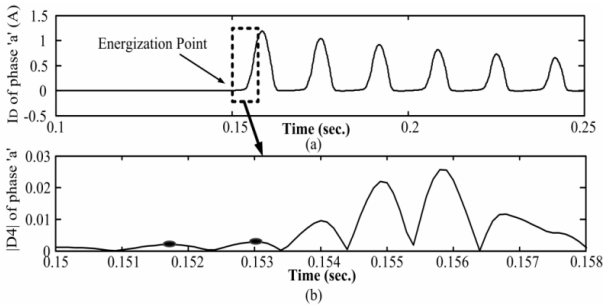


**Fig. 11.** (a) Compensated differential current of phase 'a' and (b) WT coefficient |D4| in case of retard phase shift for magnetizing inrush current

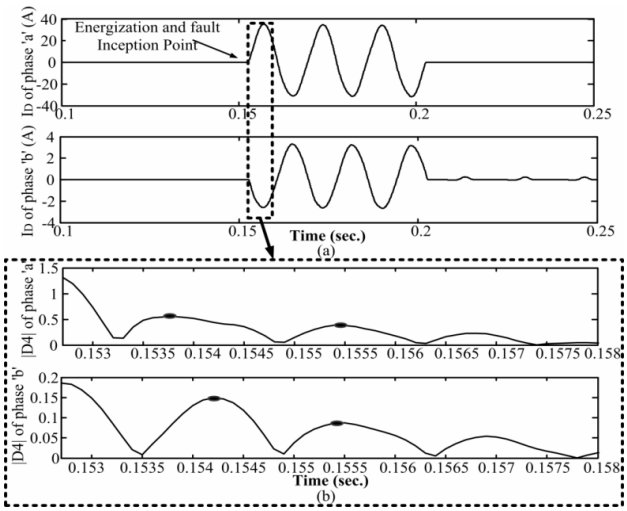


**Fig. 12.** (a) Compensated differential currents of Phase 'a' and 'b'; (b) its WT coefficient |D4| for simultaneous A-G fault and inrush condition at t=0.1527 sec

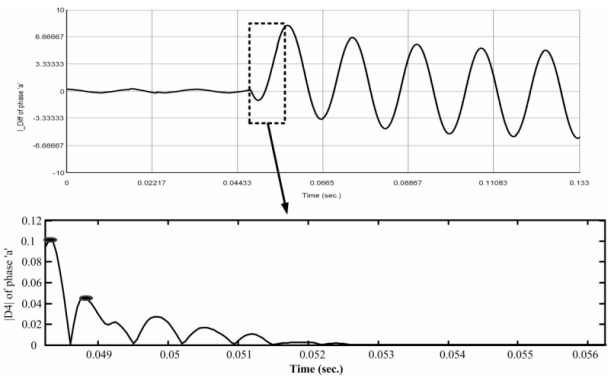


**Fig. 13.** Compensated differential currents of Phase 'a' and its WT coefficient |D4| for A-G fault in series unit secondary winding in case of advance phase shift at t=0.04825 sec

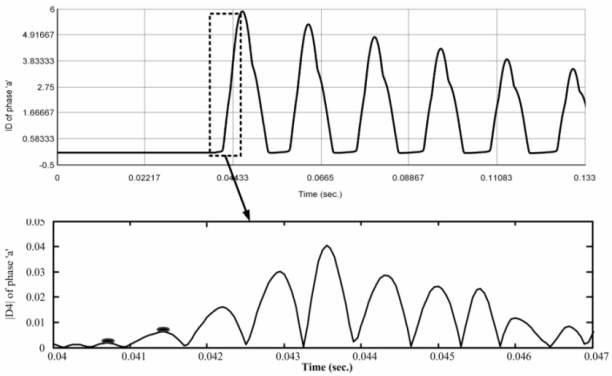


**Fig. 14.** Compensated differential current of phase 'a' and its WT coefficient |D4| in case of retard phase shift for magnetizing inrush current at t=0.04 sec

from RSCAD / RTDS software. Fig. 13 shows the compensated differential current of phase 'a' and its WT coefficient |D4| for A-G internal fault in series unit secondary winding at time t = 0.04825 sec. It is clear from the Figure that value of (X-Y) is +ve and detection time is less than a quarter cycle. Similarly, Fig. 14 shows the compensated differential current of phase 'a' and its WT coefficient |D4| for magnetizing inrush condition at time t=0.04 sec, the positive value of (X-Y) verify the proposed algorithm

### *D. Comparison of WT with Harmonic Restraint (HR) method*

In the current work, DFT-based harmonic restrained method has also been applied to compare its performance with the proposed WT based algorithm. Fig. 15 (a) and (b) show the ratio of magnitude of second harmonic to fundamental of the compensated differential current under typical internal fault and magnetizing inrush condition respectively. It is clear from the Fig. 15 that the ratio of magnitude of second harmonic to fundamental in an internal fault condition attains greater magnitude than the magnetizing inrush condition during first cycle. Therefore to avoid false tripping, the relay is blocked for one cycle which causes delay (one cycle or more than one cycle) in tripping decision. Further the HR method fails to take decision in fluctuating ratio of second harmonic to fundamental of the compensated differential current due to different loading conditions, severity of internal fault and switching-in angle. The proposed WT based algorithm has been successfully tested for these conditions. As explained in section IV and shown in figures, WT based algorithm takes the trip decision in less than a quarter cycle which justifies the use of WT based approach for reliable relay operation.

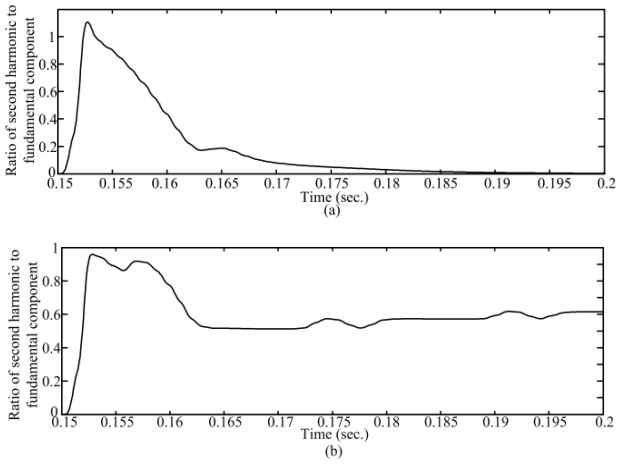


**Fig. 15.** Ratio of second harmonic to fundamental of the differential current under typical (a) internal fault condition; (b) magnetizing inrush condition occurs at 0.15 sec

## 5. Conclusion

This paper presents a novel wavelet based algorithm for the discrimination of magnetizing inrush from internal fault condition of an ISPST. This algorithm utilizes the signature of compensated differential current to discriminate magnetizing inrush from internal fault condition of an ISPST. The proposed algorithm compares magnitude of consecutive peaks of WT coefficient D4 of differential current of an ISPST. The WT coefficient D4 is preferred for diagnostic purpose over coefficient (D1-D3) as it has high comparative amplitude. Results indicate that the amplitude of coefficient D4 increases in case of inrush condition while it decreases when an internal fault occurs. The proposed algorithm is applied for many possible operating conditions of an ISPST. The proposed scheme has an operating time less than a quarter cycle. The proposed algorithm has been verified for the data generated from RSCAD/RTDS software. It is concluded that similar to power transformer, WT can also be used for differential protection of an ISPST.

## References

[1] J. Verboomen, D. Van Hertem, P. Schavemaker, W. Kling, and R. Belmans, "Phase Shifting Transformers: Principles and Applications," in *Proc. 2005 IEEE Digital Object Identifier Conf.*, pp. 1-6.

[2] J. Blade and A. Montoya, "Experiences with parallel EHV phase shifting transformers," *IEEE Trans. Power Delivery*, vol. 6, no. 3, pp. 1096-1100, July 1991.

[3] IEEE Power system relaying Committee, "Protection of Phase Angle Regulating Transformers," pp. 1-58 Oct. 1999.

[4] M. A. Ibrahim and F. P. Stacom, "Phase angle regulating transformer protection," *IEEE Trans. Power Delivery*, vol. 9, no. 1, pp. 394-404, Jan. 1994.

[5] R. A. Hedding, "Some Old and new thoughts on Phase angle Regulator Protection," in *Proc. Protective Relay Engineers 63th IEEE Annual Conf.*, pp. 1-13, Mar. 2010.

[6] M. A. Rahman, and B. Jeyasurya, "A state-of-the-art review of transformer protection algorithms," *IEEE Trans. Power Delivery*, vol. 3, no. 2, pp. 534-544, Apr. 1988.

[7] M. Tripathy, R. P. Maheshwari, and H. K. Verma, "Advances in transformer protection: A review," *Elect. Power Component Syst.*, vol. 33, no. 11, pp. 1203-1209 Aug. 2006.

[8] A. G. Phadke, and J. S. Thorp, "A new computer based flux-restrained current differential relay for power transformer protection," *IEEE Trans. on Power App. Syst.*, vol. PAS-102, no. 11, pp. 3624-3629, Nov. 1983.

[9] T. S. Sidhu, M. S. Sachdev, H. C. Wood, and M. Nagpal, "Design, implementation and testing of a

micro-processor-based high-speed relay for detecting transformer winding faults," *IEEE Trans. Power Delivery*, vol. 7, no.1, pp.108-117, Jan. 1992.
[10] M. R. Zaman, and M. A. Rahman, "Experimental testing of the artificial neural network based protection of power transformer," *IEEE Trans. Power Delivery*, vol. 13, no. 2, pp. 510-517, Apr. 1998.
[11] M. C. Shin, C. W. Park, and J. H. Kim, "Fuzzy logic based relaying for large power transformer protection," *IEEE Trans. Power Delivery*, vol. 18, no. 3, pp. 718-724, July 2013.
[12] T. Hayder, U. Schaerli, K. Feser, and L. Schiel, "Universal adaptive differential protection for regulating transformers," *IEEE Trans. Power Delivery*, vol. 23 no. 2, pp. 568-575, Apr. 2008.
[13] Z. Gajic, "Use of Standard 87T Differential protection for special three-phase power transformers-Part I: Theory," *IEEE Trans. Power Delivery*, vol. 27, no. 3, pp. 1035-1040, July 2012.
[14] B. Kasztenny, and E. Rosolowski, "Modeling and Protection of Hexagonal Phase-Shifting Transformers — Part II: Protection," *IEEE Trans. Power Delivery*, vol. 23 no. 3, pp. 1351-1358, July 2008.
[15] U. N. Khan, and T. S. Sidhu, "Protection of standard-delta phase shift transformer using terminal currents and voltages," *Elect. Power Syst. Res.*, vol. 110, pp. 31-38, May 2014.
[16] U. N. Khan, and T. S. Sidhu, "New algorithm for the protection of delta-hexagonal phase shifting transformer," *IET Gener. Transm. Distrib.*, vol. 8 no. 1, pp. 178-186, 2014.
[17] M. Geethanjali, S. M. R. Slochanal, and R. Bhavani, "PSO trained ANN based differential protection scheme for power transformers," *4th Int. Symposium on Neural Network: Algorithms and Applications*, vol. 71, no. 4, pp. 904-918, Apr. 2007.
[18] Z. Moravej, D. N. Vishwakarma, and S. P. Singh, "ANN-based protection scheme for power transformer," *Elect. Machine and Power Syst.*, vol. 28, no. 9, pp. 875-884, Nov. 2010.
[19] Z. Moravej, A. A. Abdoos, and M. Sanaye-Pasand, "Power transformer protection using improved S-transform," *Elect. Power Compon. Syst.*, vol. 39, no. 11, pp. 1151-1174, Aug. 2011.
[20] S. R. Samantaray, B. K. Panigrahi, P. K. Dash, and G. Panda, "Power transformer protection using S-transform with complex window and pattern recognition approach," *IET Gener. Transm. Distrib.*, vol. 1, no. 2, pp. 278-286, Mar. 2007.
[21] S. A. Saleh, and M. A. Rahman, "Modeling and Protection of a Three-Phase Power Transformer Using Wavelet Packet Transform," *IEEE Trans. Power Delivery*, vol. 20, no. 2, pp. 1273-1282, Apr. 2005.
[22] S. Sendil kumar, B. L. Mathur, and J. Henry, "Differential Protection for Power Transformer Using Wavelet Transform and PNN," *Electrical Power & Energy Systems Engin.*, vol. 3, no. 3, pp. 458-474, 2010.
[23] J. Faiz, and S. Lotfi-Fard, "A Novel Wavelet-Based Algorithm for Discrimination of Internal Faults From Magnetizing Inrush Currents in Power Transformers," *IEEE Trans. Power Delivery*, vol. 21, no. 4, pp. 1989-1996, Oct. 2006.
[24] Y. Y. Hong, and C. W. Wang, "Switching detection/classification using discrete wavelet transform and self-organizing mapping network," *IEEE Trans. Power Delivery*, vol. 20, no. 2, pp. 1662-1668, Apr. 2005.
[25] T. M. Lai, L. A. Snider, E. Lo, and D. Sutanto, "High-impedance fault detection using discrete wavelet transform and frequency range and RMS conversion," *IEEE Trans. Power Delivery*, vol. 20, no. 1, pp. 397-407, Jan. 2005.
[26] O. A. S. Youssef, "A wavelet-based technique for discrimination between faults and magnetizing inrush currents in transformers," *IEEE Trans. Power Delivery*, vol. 18, 1, pp. 170-176, Jan. 2003.
[27] Z.-L. Gaing, "Wavelet-based neural network for power disturbance recognition and classification," *IEEE Trans. Power Delivery*, vol. 19, no. 4, pp. 1560-1568, Oct. 2004.
[28] H. Monsef, S. Lotfi-Fard, "Internal fault current identification based on wavelet transform in power transformers," *Elect. Power Syst. Res.*, vol. 77, no. 12, pp. 1637-1645, Oct. 2007.
[29] A. Guzman, S. Zocholl, G. Benmouryal, H. J. Altuve, "A current based solution for transformer differential protection — Part I: Problem statement," *IEEE Trans. Power Delivery*, vol. 16, no. 4, pp. 485-491, Oct. 2001.
[30] U. N. Khan, "Modeling and protection of phase shifting Transformers," Doctor Thesis, Department of electrical and computer engineering, The University of Western Ontario London, Ontario, Canada 2013.

**Shailendra Kumar Bhasker** received the M.Tech. degree in Power Systems from the National Institute of Technology (NIT), Jamshedpur, in 2010. Currently, he is pursuing Ph.D. at IIT Roorkee at IIT Roorkee, India. (U.K). His research interest includes power system Protection.

**Manoj Tripathy** received the Ph.D. degree in power system engineering from Indian Institute of Technology, Roorkee (IITR), India, in 2007. Currently he is Associate Professor in the Department of Electrical Engineering, Indian Institute of Technology, Roorkee. His research interest includes Power

System Protection, Digital/Numerical Relays and Artificial Intelligence Based Relays.

**Vishal Kumar** received the Ph.D. degree in power system engineering from Indian Institute of Technology, Roorkee (IITR), India, in 2007. Currently he is Associate Professor in the Department of Electrical Engineering, Indian Institute of Technology, Roorkee. His research interest includes power distribution system, operation and control, digital design and verification.